Desalination and Water Treatment
www.deswater.com
doi: 10.1080/19443994.2013.780767

51 (2013) 6194–6200
September

Taylor & Francis
Taylor & Francis Group

Fabrication of ultra-thin polyelectrolyte/carbon nanotube membrane by spray-assisted layer-by-layer technique: characterization and its anti-protein fouling properties for water treatment

Lei Liu[a], Moon Son[a], Sudip Chakraborty[b], Chiranjib Bhattacharjee[b], Heechul Choi[a,*]

[a]*School of Environmental Science and Engineering, Gwangju Institute of Science and Technology (GIST), 261 Cheomdan-gwagiro, 1 Oryong-dong, Buk-gu, Gwangju 500-712, South Korea*
Tel. +82 62 7152576; Fax: +82 62 7152434; email: hcchoi@gist.ac.kr
[b]*Department of Chemical Engineering, Jadavpur University, 188, Raja Subodh Chandra Mullick Road, Kolkata 700-032, India*

Received 10 October 2012; Accepted 10 December 2012

ABSTRACT

Polyethersulfone (PES) membranes are extensively used as ultrafiltration (UF) membrane owing to their superior thermal, mechanical, and chemical stability. However, commercial PES membranes are more prone to fouling, which contributes to severe decline in permeate flux with operation time. To improve the commercial PES UF membrane anti-protein fouling properties, negatively charged functionalized multi-walled carbon nanotube (f-MWCNTs), blended poly(sodium 4-styrenesulfonate) (PSS), and positively charged poly(diallyldimethylammonium chloride) (PDDA) were deposited on 20 kDa PES substrate through spray-assisted layer-by-layer (LbL) technique. Further cross-flow UF tests were conducted with bovine serum albumin (BSA) as model protein. The total flux loss results show that surface-modified PES membranes are less susceptible to protein fouling by one-hour BSA filtration. Moreover, flux recovery ratios show that 20-min de-ionized (DI) water flushing is effective to restore water flux of the prepared membrane without aggressive chemical cleaning. Based on the experimental results, the excellent anti-fouling properties render the prepared membranes suitable for recycling utilization.

Keywords: Anti-fouling; Ultrafiltration (UF); Layer-by-layer (LbL); Carbon nanotube (CNTs)

1. Introduction

Ultrafiltration (UF) is a pressure-driven membrane process to retain macromolecules or high molecular-weight compounds, excluding bacteria and viruses. It is characterized by low energy consumption, high water output, compact installation, and easy automation [1]. To date, UF is considered as one of the promising alternative in water reclamation to produce qualified and drinkable water [2].

In spite of many advantages, flux decline resulted from membrane fouling is the most serious and inherent obstacle for the efficient application of UF process

*Corresponding author.

Presented at The Fifth Desalination Workshop (IDW 2012), October 28–31, 2012, Jeju, Korea

[3]. UF membrane fouling can be generally categorized into two types: (1) macrosolute adsorption, which is usually irreversible, adhesive fouling and (2) cake formation, which is often reversible, nonadhesive fouling [4]. Cake formation is easily overcome by water flushing or back washing [5]. In contrast, irreversible fouling exhibited a marked dependence on membrane surface chemistry, such as roughness, electrostatic charge [6]. Aside from other foulants, protein fouling is a critical problem for UF process and widely reported [7–10]. In protein fouling mechanism studies, bovine serum albumin (BSA) is often chosen as a model protein [11].

Among various surface modification methods, layer-by-layer(LbL) approach is a versatile technique to enable fine control and tunable fabrication of thin multilayer made of diverse components, such as polymers, small molecules, and inorganic materials without the constraints [12]. The LbL approach encompasses deposition on a substrate in sequences of alternating charge or other secondary interactions [13]. Spray-assisted LbL technique surpasses the conventional dip-coating LbL method for the reason that it is suited for a large-scale production and time and material savings without affecting the coated layer's quality [14]. Polyelectrolyte, which is frequently used in LbL process, is a water-soluble polymer and dissociates in aqueous solutions making the polymers charged (polysalts) [15]. The polyelectrolyte polymer chain exists in an almost fully extended, rodlike configuration in the absence of salt in solution [16], therefore, the roughness of substrate modified by polyelectrolyte will be mitigated by polyelectrolyte multilayer deposition [17], then influence the adhesion of foulants.

Previous studies have proven that multi-walled carbon nanotubes (MWCNTs) have an exceptionally high aspect ratio in combination with low density, high strength, and stiffness, which makes them a potential candidate as an effective reinforcing additive in polymeric materials [18]. However, raw CNTs' physical properties, such as small diameter in nanometer scale with high aspect ratio (>1,000), extremely large surface area, and heavily entangled bundles result in CNTs processing difficulties and poor interfacial interaction between CNTs and polymer matrix [19]. The functionalization process is necessary for CNTs to disentangle, open up the tubes, remove the impurities during chemical vapor deposition process, and provide functional groups (carboxyl and hydroxyl groups) on CNTs tips and sidewalls [20]. Poly(sodium 4-styrenesulfonate) (PSS) is a facile and effective polymer to assist in the dispersion of f-MWCNTs in aqueous solutions [21], consequently, incorporation of f-MWCNTs into PSS solution imparts the enhanced negative charge density to PSS layer, hence, increase electrostatic repulsion of anionic foulants.

Polyelectrolyte multilayer membranes were prepared and used for ion separation, organic removal, and solvent resistant nanofiltration [22]. However, limited studies have been conducted to explore polyelectrolyte/f-MWCNTs membranes in water treatment and their anti-protein fouling tests. In this study, f-MWCTNs' blended polyelectrolyte membranes are fabricated via spray-assisted LbL technique; attempts will be made to explain the anti-protein fouling properties results from surface property changes after bare Polyethersulfone (PES) membrane surface modification.

2. Experimental

2.1. Materials

The PES substrate (PES20, 20,000 Da) was obtained from AMFOR INC., USA. MWCNTs were purchased from Hanwha Nanotech. Co. Ltd., Korea. PSS (Mw = 70,000 Da, powder, Sigma-Aldrich, USA) and poly (diallyl-dimethylammonium chloride) (PDDA, Mw = 100,000–200,000 Da, 20 wt% in H_2O, Sigma–Aldrich, USA) were used as received. BSA (Mw = 68,000 Da) with isoelectric point (IEP) at pH 4.7–4.9 was provided by Roche, Switzerland. De-ionized (DI) water (Milli-Q, 18.2 MΩcm) was used for rinsing and solutions preparation.

2.2. Functionalization of MWCNTs

MWCNTs functionalization method was described elsewhere [23,24]. The morphology of functionalized MWCNTs (f-MWCNTs) was analyzed by transmission electron microscopy (TEM, JEM-2100, JEOL, Japan) and the functional groups on MWCNTs were detected by fourier transform spectroscopy (FTIR-460 plus, JASCO, Japan).

2.3. Polyelectrolyte multilayer membrane fabrication and characterization

The f-MWCNTs were added to 20% (v/v) ethanol aqueous solution and ultrasonicated for 30 min, then PSS aqueous solution was mixed with MWCNTs solution to form 1 mg/mL homogenous PSS solution with 1% (CNT/polymer w/w) MWCNTs content with the aid of another 10 min ultrasonication. 1 mg/mL PDDA aqueous solution was prepared by spiking the PDDA polymer into DI water. Both PSS and PDDA aqueous solution were prepared without adjusting the pH for the reason that both polymers are strong polyelectrolytes and can be fully ionized in a wide pH range [17].

Prior to deposition process, the PES substrates were soaked in 25 °C DI water for 24 h as recommended by the supplier to fully remove the wetting agent of the membrane, during which the water was replaced every three hours. The pretreated PES membrane was mounted on a holder so that only one side of PES membrane contacted with the spraying solution.

The fabrication of polyelectrolyte multilayer membrane via spray-assisted technique was fulfilled under 20 psi of compressed air by spray pistol (GP-1, 0.35 mm nozzle diameter, Fuso SEIKI Co., Ltd., Japan), the scheme is illustrated in Fig. 1. The process repeated n cycles, that is, n bilayers of PSS/MWCNTs-PDDA thin film were formed on the PES membrane. Spraying was initiated by PSS/MWCNTs on the PES substrate through hydrogen bonding, hydrogen-hydrogen, and hydrophobic interactions [25,26], the positively charged PDDA interact with PSS/MWCNTs layer via electrostatic and van der Waals forces [25]. All the membranes are freshly prepared before use.

Roughness of membranes was measured by atomic force microscope (AFM, XE-100, PSIA, Korea) in a contact mode with a scan size of 2 μm × 2 μm.

2.4. Anti-fouling UF test

UF test was carried out by homemade cross-flow filtration test unit equipped with temperature controller, operating flow rate meter, and pressure gage. All the membranes were stabilized at transmembrane pressure (TMP) of 0.41 Mpa for 4 h, then the pressure was adjusted to 0.35 Mpa operating TMP. In order to evaluate the membrane anti-fouling properties, water flushing at a flow rate of 36 L/h for 20 min was followed by 1 mg/mL BSA aqueous solution filtration performed at 25 ± 1℃ for 1 h, the pH was maintained by 10 mM phosphorus buffer at pH 7.

The water flux of virgin membrane (J_{wv}), fouled membrane (J_{pf}) after one-hour BSA filtration, and cleaned membrane (J_{wp}) after water flushing were determined using

$$J = \frac{V}{A\Delta t} \tag{1}$$

where V is the volume of permeated water (L), A is the effective membrane area ($1.856 \times 10^{-3}\,m^2$), and $\triangle t$ is the permeation time (h). At the same time, the flux recovery ratio (FRR) and total flux loss R_t, which are assumed to be measured for fouling resistance nature of membrane [27], are calculated using the formula:

$$\mathrm{FRR}\ (\%) = \left(\frac{J_{wp}}{J_{wv}}\right) \times 100\% \tag{2}$$

$$R_t\ (\%) = \left(\frac{J_{wv} - J_{pf}}{J_{wv}}\right) \times 100\% \tag{3}$$

The BSA rejection R was calculated by

$$R\ (\%) = \left(1 - \frac{C_p}{C_f}\right) \times 100\% \tag{4}$$

where C_p and C_f are the concentrations of BSA in the feed and permeate, respectively.

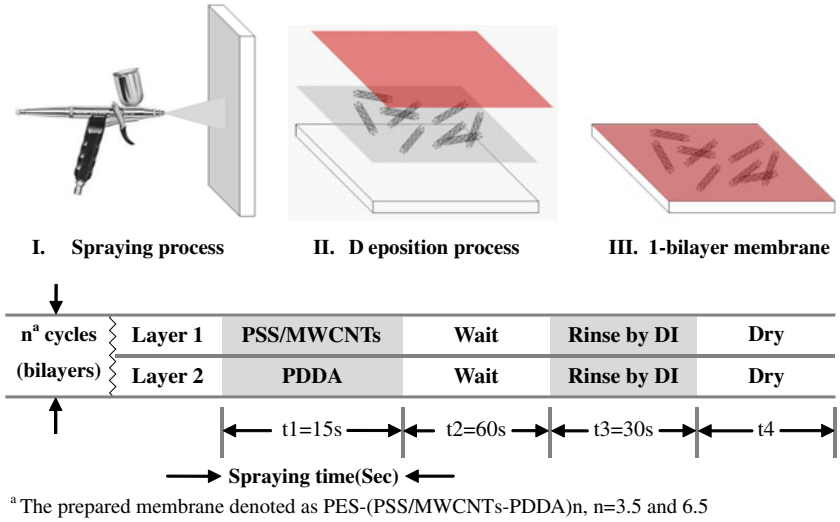

[a] The prepared membrane denoted as PES-(PSS/MWCNTs-PDDA)n, n=3.5 and 6.5

Fig. 1. Scheme for the fabrication of polyelectrolyte multilayer membrane via spray-assisted technique.

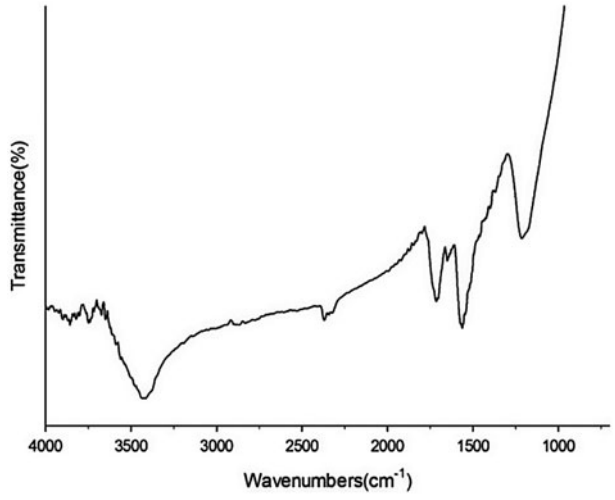

Fig. 2. The FTIR spectrum of f-MWNCTs.

3. Results and discussion

3.1. Characterization of functionalized MWCNTs

The FTIR spectrum of functionalized MWCNTs is shown in Fig. 2. The absorption band at around 3,416 cm^{-1} is assigned to –OH group [28], whereas, bands at 1,713 and 1,647 cm^{-1} are attributed to C=O stretching vibration [29,30]. The peak around 1,563 and 1,214 cm^{-1} indicate the C=C ring stretching of MWCNTs and –C–O group [31,32], respectively. The FTIR spectrum confirms that MWCNTs are functionalized with hydroxyl and carboxylic groups after chemical modification by mixed acid.

TEM images show the morphology changes of the MWCNTs before and after functionalization (Fig. 3). It is obvious for raw commercial MWCNTs that entangled and coiled ropes of nanotubes are observed. After functionalization, the lengths of MWCNTs are shortened to ~400 nm with both tips open, and the functionalized MWCNTs are well dispersed in aqueous solution with the assist of ethanol.

3.2. Membrane characterization

AFM results (Fig. 4) clearly indicate the morphological changes of bare PES membrane before and after surface modification. PES membrane surface deposition by polyelectrolyte/MWCNTs on the membrane surface results in a smoother surface than the bare PES membrane, the PES-(PSS/MWCNTs-PDDA) 6.5 membrane exhibited the least roughness compared to other membranes.

3.3. Anti-fouling UF

Since UF is a pressure-driven process, Fig. 5 demonstrates the linear relationship between pure water flux of membrane and TMP. Meanwhile, with more bilayer deposition on PES substrate, the flux decrease accordingly, which suggests the successful deposition of the polyelectrolyte multilayer on PES substrate.

The membrane anti-fouling properties are examined by total flux loss R_t and flux recovery ratio (FRR). After 6.5 bilayer deposition, R_t decreases from 64% for bare PES membrane to 28%, in addition, the FRR of 88% is obtained comparing to 51% for unmodified PES membrane (Fig. 6). This result is consistent with earlier studies on improved anti-fouling properties by PSS-modified PES membrane [27].

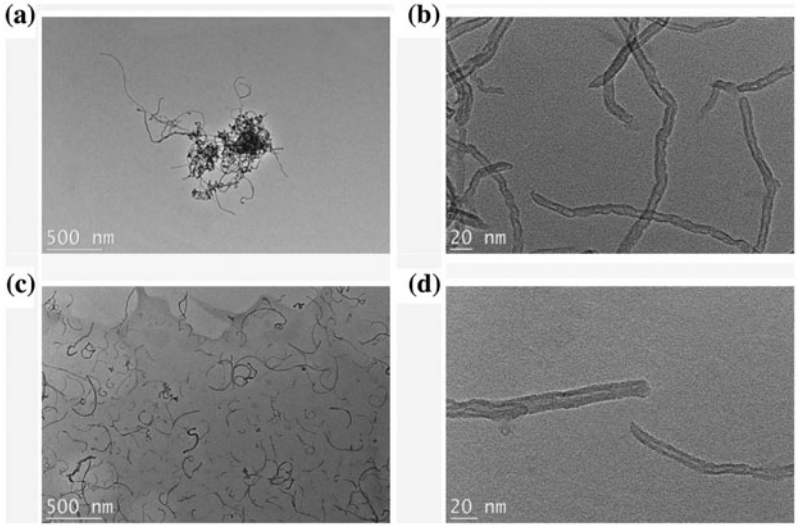

Fig. 3. TEM images of (a, b) raw MWCNT and (c, d) functionalized MWNCT.

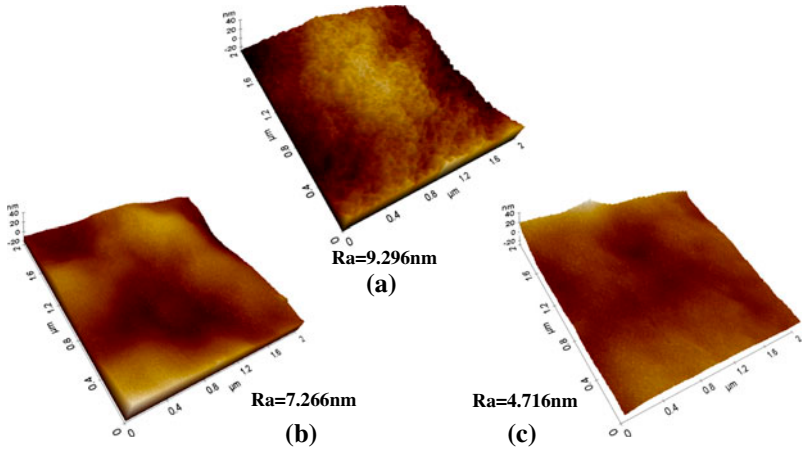

Fig. 4. Tapping mode AFM images of the prepared membranes (a) bare PES membrane, (b) 3.5 bilayer deposition, and (c) 6.5 bilayer deposition.

To further differentiating parameters contributing to the total flux loss R_t and FRR, the revisable (R_r) and irreversible (R_{ir}) ratios are introduced and defined using the following equation:

$$R_r = \left(\frac{J_{wp} - J_{pf}}{J_{wv}}\right) \times 100\% \quad (5)$$

$$R_{ir} = \left(\frac{J_{wv} - J_{wp}}{J_{wv}}\right) \times 100\% \quad (6)$$

The increasing number of bilayer gives rise to significant reduction in the irreversible ratio and a slight increase in the reversible ratio and rejections (Table 1).

Basically, the rejection of BSA is governed by size exclusion due to the molecular weight of BSA being much larger than the MWCO of the tested membrane. Interactions between charged foulants and the membrane can be reduced by enhancing electrostatic repulsion through altering the membrane surface charge [33]. The introduction of the negatively charged f-MMWCTs in the polyelectrolyte multilayer exerts enhanced negative charge density on the membrane surface, BSA is also negatively charged under operating pH 7 as the pH is higher than IEP. Thus, the prepared membrane surface leads to indirect contact or loosely BSA adhesion. On top of that, AFM images display a smoother surface after deposition, which is beneficial for anti-fouling [34]. Hence, Fig. 6 and Table 1 show as the deposition layer increases, the higher R_t, R_{ir}, and FRR can be achieved. The increased rejection for BSA can be explained by size exclusion and charge repulsion.

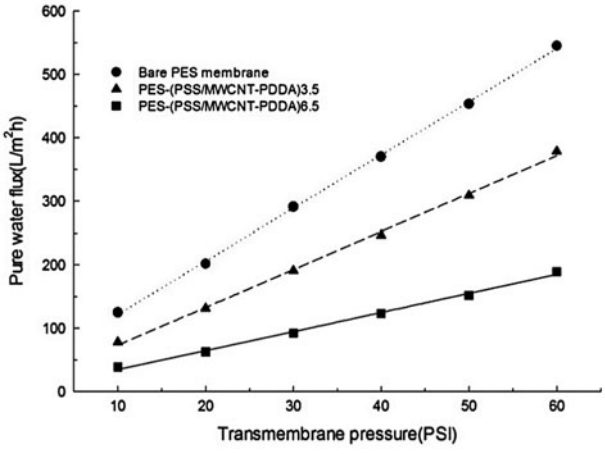

Fig. 5. Pure water flux of the polyelectrolyte multilayer membranes as a function of the TMP.

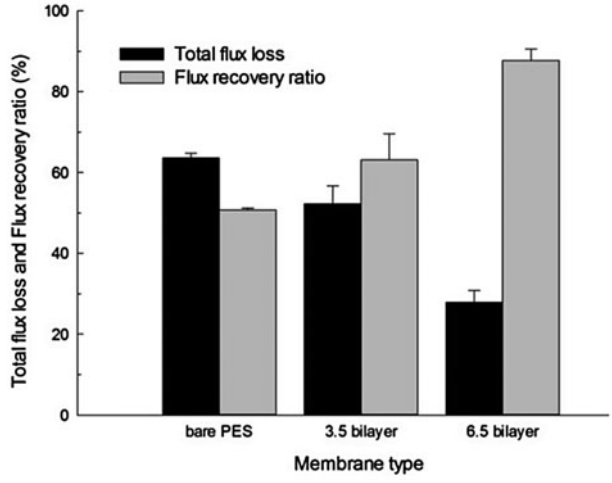

Fig. 6. Flux loss and recovery of the prepared membranes for anti-fouling test (average results and standard deviation of two replicates are reported).

Table 1
Fouling ratios of the prepared membrane for anti-fouling test (average results and standard deviation of two replicates are reported)

Membrane type	Fouling ratios of BSA (%)		Rejection (%)
	R_{ir}	R_r	
Bare PES	49.3 ± 0.5	14.3 ± 0.7	99.78 ± 0.07
PES-(PSS/MWCNT-PDDA)3.5	36.9 ± 6.5	15.4 ± 2.0	99.84 ± 0.12
PES-(PSS/MWCNT-PDDA)6.5	12.3 ± 2.9	15.5 ± 0.1	99.90 ± 0.08

4. Conclusion

According to the experimental results, the following conclusions can be drawn:

(1) PES-polyelectrolyte/MWCNTs membrane was prepared through spray-assisted layer-by-layer technique, which is versatile, time-saving, and promising for large-scale productions.
(2) 3.5 and 6.5 bilayer deposition of polyelectrolyte/MWCNTs on PES substrate render the membrane with excellent anti-protein fouling and flux recovery properties. The membranes are expected to be utilized in a recycling way by simple water flushing.
(3) Further membrane characterization and anti-bacterial properties of the prepared membrane need to be studied.

Nomenclature

A	—	effective membrane area
BSA	—	bovine serum albumin
C_f	—	concentration of BSA in the feed
C_p	—	concentration of BSA in the permeate
f-MWCNTs	—	functionalized MWCNTs
FRR	—	flux recovery ratio
IEP	—	isoelectric point
J_{pf}	—	water flux of fouled membrane after one-hour BSA filtration
J_{wp}	—	water flux of cleaned membrane after water flushing
J_{wv}	—	water flux of virgin membrane
LbL	—	layer-by-layer
MWCNTs	—	multi-walled carbon nanotube
PDDA	—	poly(diallyldimethyl-ammonium chloride)
PES	—	polyethersulfone
PSS	—	poly(sodium 4-styrenesulfonate)
R	—	BSA rejection
R_{ir}	—	flux irreversible ratio
R_r	—	flux revisable ratio
R_t	—	total flux loss
TMP	—	trans membrane pressure
UF	—	ultrafiltration
V	—	volume of permeated water
Δt	—	permeation time

Acknowledgments

This work was supported by the National Research Foundation of Korea (NRF) grant funded by the Korea government (MEST) (Nos. 2011-0027712 and 2012R1A2A2A03046711) and "Basic Research Projects in High-tech Industrial Technology" Project through a grant provided by GIST in 2013.

Reference

[1] J.M. Arnal, M. Sancho, G. Verdú, J. Lora, J.F. Marín, J. Cháfer, Selection of the most suitable ultrafiltration membrane for water disinfection in developing countries, Desalination 168 (2004) 265–270.
[2] W. Gao, H. Liang, J. Ma, M. Han, Z.-l. Chen, Z.-s. Han, G.-b. Li, Membrane fouling control in ultrafiltration technology for drinking water production: A review, Desalination 272 (2011) 1–8.
[3] L. Gzara, M. Dhahbi, Removal of chromate anions by micellar-enhanced ultrafiltration using cationic surfactants, Desalination 137 (2001) 241–250.
[4] N. Hilal, O.O. Ogunbiyi, N.J. Miles, R. Nigmatullin, Methods employed for control of fouling in MF and UF membranes: A comprehensive review, Sep. Sci. Technol. 40 (2005) 1957–2005.
[5] R. Baker, Membrane Technology and Applications, John Wiley, Chichester, 2012.
[6] M. Taniguchi, J.E. Kilduff, G. Belfort, Low fouling synthetic membranes by UV-assisted graft polymerization: Monomer selection to mitigate fouling by natural organic matter, J. Membr. Sci. 222 (2003) 59–70.
[7] K.L. Jones, C.R. O'Melia, Protein and humic acid adsorption onto hydrophilic membrane surfaces: Effects of pH and ionic strength, J. Membr. Sci. 165 (2000) 31–46.
[8] T. Maruyama, S. Katoh, M. Nakajima, H. Nabetani, T.P. Abbott, A. Shono, K. Satoh, FT-IR analysis of BSA fouled on ultrafiltration and microfiltration membranes, J. Membr. Sci. 192 (2001) 201–207.
[9] S. Boributh, A. Chanachai, R. Jiraratananon, Modification of PVDF membrane by chitosan solution for reducing protein fouling, J. Membr. Sci. 342 (2009) 97–104.
[10] Y.-N. Wang, C.Y. Tang, Protein fouling of nanofiltration, reverse osmosis, and ultrafiltration membranes—The role of hydrodynamic conditions, solution chemistry, and membrane properties, J. Membr. Sci. 376 (2011) 275–282.
[11] Z.-P. Zhao, Z. Wang, S.-C. Wang, Formation, charged characteristic, and BSA adsorption behavior of carboxymethyl chitosan/PES composite MF membrane, J. Membr. Sci. 217 (2003) 151–158.
[12] J.J. Cerda, B. Qiao, C. Holm, Understanding polyelectrolyte multilayers: An open challenge for simulations, Soft Matter 5 (2009) 4412–4425.
[13] P.T. Hammond, Engineering materials layer-by-layer: Challenges and opportunities in multilayer assembly, AlChE J. 57 (2011) 2928–2940.
[14] A. Izquierdo, S.S. Ono, J.C. Voegel, P. Schaaf, G. Decher, Dipping versus spraying: Exploring the deposition conditions for speeding up layer-by-layer assembly, Langmuir 21 (2005) 7558–7567.

[15] D. Mecerreyes, Polymeric ionic liquids: Broadening the properties and applications of polyelectrolytes, Prog. Polym. Sci. 36 (2011) 1629–1648.
[16] R.A. McAloney, M. Sinyor, V. Dudnik, M.C. Goh, Atomic force microscopy studies of salt effects on polyelectrolyte multilayer film morphology, Langmuir 17 (2001) 6655–6663.
[17] P. Ahmadiannamini, X. Li, W. Goyens, B. Meesschaert, I.F.J. Vankelecom, Multilayered PEC nanofiltration membranes based on SPEEK/PDDA for anion separation, J. Membr. Sci. 360 (2010) 250–258.
[18] J.N. Coleman, U. Khan, W.J. Blau, Y.K. Gun'ko, Small but strong: A review of the mechanical properties of carbon nanotube–polymer composites, Carbon 44 (2006) 1624–1652.
[19] P.-C. Ma, N.A. Siddiqui, G. Marom, J.-K. Kim, Dispersion and functionalization of carbon nanotubes for polymer-based nanocomposites: A review, Composites Part A 41 (2010) 1345–1367.
[20] X.-L. Xie, Y.-W. Mai, X.-P. Zhou, Dispersion and alignment of carbon nanotubes in polymer matrix: A review, Mater. Sci. Eng. R 49 (2005) 89–112.
[21] S. Zhan, Y. Li, Noncovalent functionalization of multiwalled carbon nanotubes by anionic polymer poly(sodium 4-styrenesulfonate) in water, J. Dispersion Sci. Technol. 29 (2008) 240–244.
[22] L. Krasemann, B. Tieke, Selective ion transport across self-assembled alternating multilayers of cationic and anionic polyelectrolytes, Langmuir 16 (1999) 287–290.
[23] E. Celik, L. Liu, H. Choi, Protein fouling behavior of carbon nanotube/polyethersulfone composite membranes during water filtration, Water Res. 45 (2011) 5287–5294.
[24] J. Liu, A.G. Rinzler, H. Dai, J.H. Hafner, R.K. Bradley, P.J. Boul, A. Lu, T. Iverson, K. Shelimov, C.B. Huffman, F. Rodriguez-Macias, Y.-S. Shon, T.R. Lee, D.T. Colbert, R.E. Smalley, Fullerene Pipes, Science 280 (1998) 1253–1256.
[25] F. Diagne, R. Malaisamy, V. Boddie, R.D. Holbrook, B. Eribo, K.L. Jones, Polyelectrolyte and silver nanoparticle modification of microfiltration membranes to mitigate organic and bacterial fouling, Environ. Sci. Technol. 46 (2012) 4025–4033.
[26] R. Malaisamy, M.L. Bruening, High-flux nanofiltration membranes prepared by adsorption of multilayer polyelectrolyte membranes on polymeric supports, Langmuir 21 (2005) 10587–10592.
[27] A.V.R Reddy, D.J Mohan, A. Bhattacharya, V.J. Shah, P.K. Ghosh, Surface modification of ultrafiltration membranes by preabsorption of a negatively charged polymer: I. Permeation of water soluble polymers and inorganic salt solutions and fouling resistance properties, J. Membr. Sci. 214 (2003) 211–221.
[28] Y. Yu, J.C. Yu, J.-G. Yu, Y.-C. Kwok, Y.-K. Che, J.-C. Zhao, L. Ding, W.-K. Ge, P.-K. Wong, Enhancement of photocatalytic activity of mesoporous TiO2 by using carbon nanotubes, Appl. Catal. A 289 (2005) 186–196.
[29] G. Moraitis, Z. Špitalský, F. Ravani, A. Siokou, C. Galiotis, Electrochemical oxidation of multi-wall carbon nanotubes, Carbon 49 (2011) 2702–2708.
[30] F. Esnaashari, M. Moghadam, V. Mirkhani, S. Tangestaninejad, I. Mohammadpoor-Baltork, A.R. Khosoropour, M. Zakeri, S.H. Rad, MoO2(acac)2 supported on multi-wall carbon nanotubes: Highly efficient and reusable catalysts for alkene epoxidation with tert-BuOOH, Polyhedron 48 (2012) 212–220.
[31] M.-Y. Hua, Y.-C. Lin, R.-Y. Tsai, H.-C. Chen, Water dispersible 1-one-butyric acid-functionalised multi-walled carbon nanotubes for enzyme immobilization and glucose sensing, J. Mater. Chem. 22 (2012) 2566–2574.
[32] C.-F. Kuan, H.-C. Kuan, C.-C.M. Ma, C.-H. Chen, Mechanical and electrical properties of multi-wall carbon nanotube/poly (lactic acid) composites, J. Phys. Chem. Solids 69 (2008) 1395–1398.
[33] J.S. Louie, I. Pinnau, I. Ciobanu, K.P. Ishida, A. Ng, M. Reinhard, Effects of polyether–polyamide block copolymer coating on performance and fouling of reverse osmosis membranes, J. Membr. Sci. 280 (2006) 762–770.
[34] X. Cao, J. Ma, X. Shi, Z. Ren, Effect of TiO_2 nanoparticle size on the performance of PVDF membrane, Appl. Surf. Sci. 253 (2006) 2003–2010.